

MATHEMATICAL MODELLING AND EXPERIMENTAL EVALUATION OF NON-UNIFORM WATER FLOW IN FLAT PLANE SOLAR COLLECTORS

Lucas Paglioni Pataro Faria, lppf@ig.com.br

School of Engineering / Federal University of Minas Gerais / Address: Antônio Carlos Avenue, 6627, Zip Code: 31.270-901, Belo Horizonte / Minas Gerais / Brazil.

Elizabeth Marques Duarte Pereira, green@pucminas.br

Pontifical Catholic University of Minas Gerais / Address: Dom José Gaspar Avenue, 500, Building 50, Zip Code: 30.535-901, Belo Horizonte / Minas Gerais / Brazil.

Rudolf Huebner, rudolf@ufmg.br

School of Engineering / Federal University of Minas Gerais / Address: Antônio Carlos Avenue, 6627, Zip Code: 31.270-901, Belo Horizonte / Minas Gerais / Brazil.

Abstract. *The economy propitiated by the solar water heaters, in substitution to the electric showers, it is understood as a virtual generation of electric power, because these equipments are responsible for more than 5% of the national consumption of electric power and for about 18% of the top demand of the electric system. The consumption minimization would mean a great benefit for the generation system and energy distribution, moving the urgency of great investments of resources, besides, reducing the environmental pressure brought by the flood of great necessary areas to the hydroelectric ones. For the intensive implementation of solar heating systems, its becomes still necessary the development of simulation tools that allow a discerning analysis of the solar collectors behavior in associations of great load, activating the project stage and inserting the collectors in these associations with larger reliability degree. The proposed physical model bases on the equations of energy conservation, mass and momentum, contemplating the no-uniformity of the flow in the distribution tubes of the solar collectors. The developed experimental procedures include internal rehearsals accomplished in the solar simulator for thermal acting evaluation of the collector solar plan, operating under different conditions of water flow. The results obtained experimentally were used for validation of the proposed numeric model. The results analysis obtained experimentally was confronted with the numeric results, being observed the tolerances and uncertainties of the used instrumentation, being obtained quite satisfactory results for the simulation, especially for the temperature fluid distribution.*

Keywords: Energy; Solar; Heating; Simulator; Model and Numeric.

1. INTRODUCTION

The use of solar energy in large plants has been gaining space in the Brazilian market as an effective conservation of energy and reduction of operating costs. In these cases, the application of large batteries of collectors, for water heating, associated in series and parallel are required to meet the flow demands of water and temperature levels. This requires studies on total efficiency of the collectors association, depending on the individual efficiency of the equipment and the water flow uniformity in their batteries of solar collectors. Several authors have developed studies on the evaluation of various parameters that influence the efficiency of a collector or an association of collectors. Simon (1976) uses a solar simulator to determine the efficiency of solar collectors to ensure controlled conditions of wind, temperature and solar irradiation. Their results validate the internal tests and demonstrate that a simple reduction in the heat loss does not guarantee better efficiency of the solar collector. Cooper and Dunkle (1981) propose a nonlinear model for a solar collector, but consider that the overall coefficient of heat loss varies linearly with the temperature difference between fluid in the collector and the environment, typical of facilities in series. Chiou (1982) considers the flow distribution in the pipes is usually non-uniform in the elevation tubes under normal operation conditions. This condition may be associated with imperfections in construction, improper installation of solar collectors or deposition problems and clogging of the pipes. In their work, are considered sixteen models with inadequate flow distribution. The degradation of the collector efficiency due the effects of flow non-uniformity is determined for several collectors in terms of production / operation. Conclusively a parameter of flow non-uniformity " Φ " is introduced to represent the differences of the flow bad distribution in relation to its principal value. It was found in this study a unique relationship between the deterioration degree of the collector efficiency due the effect of their flow non-uniformity and the parameter of flow non-uniformity Φ . Oliva *et al.* (1991) propose a numerical model for determining the thermal behavior of a solar collector. The model takes into account the multidimensional and transients aspects that characterize the phenomenon of heat transfer in a solar collector. The model allows the analysis of the influence of things like: non-uniform distribution of flow, areas of shading and variations in size and properties of different elements. Kang M. *et al.* (2006) prepared a numerical model to study the thermal performance of a large association of solar collectors, which can be

integrated as part of the structure of a roof, without major difficulties. According to the authors, the combination of solar collectors is a network of elevation tubes and manifolds to simulate collectors connected in series, forming a major collector. The results show that the thermal efficiency of the association of collectors is mainly influenced by the amount of elevation tubes, where the ratio H is the length of the elevation tube and W is the width of the solar collector, the mass flow rate, thermal conductivity and thickness of the absorber plate. Differences in the range 2.5 to 8.0% were detected, depending on the particular parameter tested. One of the conclusions of the author is that the water in the dividing manifolds remains nearly at the same temperature to the input of the solar collector, although there is some heat transfer through the walls of the elevation tubes. The physical model, developed by (Wang and Wu, 1990), discuss the non-uniformity of water flow in the distribution pipes (branch pipes). The system of equations generated based on the laws of conservation of mass, momentum and energy is composed of 19 equations for each tube and was used as reference in the development of this work. The contribution of this work, in supplement to previous studies prepared by other authors, deals with the development of a behavior analysis of solar collectors in large associations, with the creation of simulation tools that speed up the stage of design and integration of collectors in these associations with a higher degree of reliability. The purpose of this work is the development of a mathematical model to assess the overall efficiency compared to solar collectors taking into account the effects of flow non-uniformity of the water through the distribution pipes and validate the model developed from the comparison between the results of mathematical simulations and experimental trials.

2. MATHEMATICAL MODELING

The analysis and calculations have been developed initially for only in one elevation tube of the distribution pipes, despite the solar collector set to study has a total of seven elevation tubes, based on the theories of heat transfer and mechanics of fluids. Thus, the methodology, the sequence of calculations and the relevant considerations are highlighted. As this elevation tube can represent a bench of n solar collectors associated in parallel there is good correlation with the actual operation of solar heating systems. The developed model was implemented in the programs Engineering Equations Solver (EES) and Matlab.

2.1. Velocities distribution in the distribution pipes and dividing manifold

The model developed is based on the theory described in the Hardy Cross Model. Adopted the specified flow by international standards for testing solar collectors, pr EN 12975-2 and ANSI / ASHRAE 93-2003, equal to 1.2 liters per minute per square meter of collector area. As the solar collector in question has a collector area of 1.72 m², the flow test is 3.4×10^{-5} m³/s. This value is used during all simulations performed, although for other flows, the analysis is similar.

The Hardy Cross model was used to estimate the input speeds into each of the distribution pipes ($V_{bd}(i)$) and in each dividing segments ($V_{dl}(i)$). The output speeds of each dividing segments ($V_{dr}(i)$) were considered equal to the input speeds, assuming that the flow of heat in this segments are negligible. However, the model developed in this paper that consideration was not maintained for the combining segments. At the combining segments was applied a mass balance to determining the entry and exits speeds of the water.

The output speeds were determined from the balance of mass in the same segments. In principle, it is assumed that the output speeds in the division segments will be identical to the entry speeds because the amount of energy delivered is very small and the flow can be described as isothermal in this way serves to the condition imposed by the Hardy Cross model for the dividing segments at the dividing manifold. For the combining segments we chose do not apply the Hardy Cross model. Adopted the balance of mass from the equation of momentum to calculate the water temperature at the outlet of the distribution pipes.

2.2. Resolution of governing equations for the solar collector

The methodology is to divide the solar collector in nodes and applying them in transition equations. The nodes include the dividing segments, elevation tubes and combining segments are numbered in sequence from the first elevation tube. The equations governing the behavior of the dividing e combining manifolds are called transition equations, this name comes from the fact that these equations represent the transition from the variables of the previous node to the subsequent node and also the equations are numbered in sequence from the first dividing manifold and the first combining manifold (Wang and Wu, 1990).

The equations are show only for the node $i = 0$ and the results can be used to feed the same equations in the transition and next node $i = 1$. Figure 2. illustrates the division of the nodes of the solar collector, but also the dividing segments, denoted by subscripts (dl , db and dr) and the combining segments, denoted by the subscript (cl , cr and bc). The pipeline that connects all dividing segments is called a dividing manifold and the pipeline that connects all combining segments is called the combining manifold. The pipeline that connects a dividing segment with a combining segment is called the elevation tube.

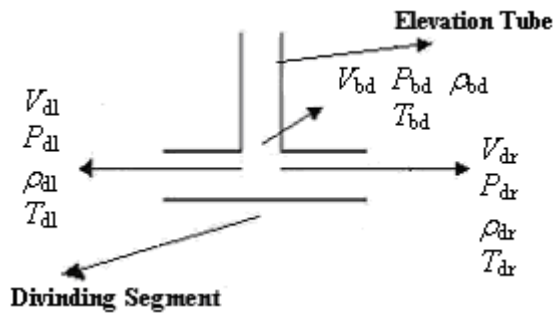


Figure 1. Dividing Segment

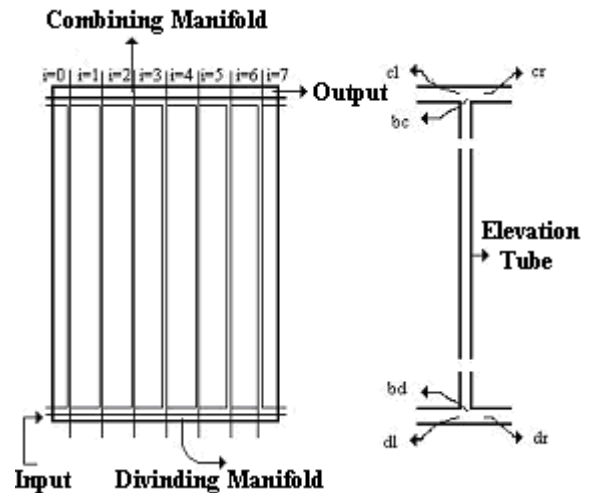


Figure 2. Simulated Solar Collector

Step 1 - Definition of temperature in the dividing segments

From the calculated flow by the Hardy Cross method (isothermal), is quite acceptable to admit that:

$$T_{bd}(i) = T_{dr}(i) = T_{dl}(i) \quad (1)$$

Where: T Temperature (K)

This condition was adopted for all dividing segments, showed in Fig. 1, therefore the input temperature of the control volume of the dividing segment $T_{dl}(i)$ is equal to the other two output temperatures for the same control volume $T_{bd}(i)$ and $T_{dr}(i)$.

Step 2 - Determination of the output temperature in the elevation tube - $T_{bc}(i)$

Using the equation for the temperature distribution in the flow direction:

$$\frac{T_f - T_a - \frac{S}{U_L}}{T_{fi} - T_a - \frac{S}{U_L}} = \exp\left(\frac{-U_L n W F' y_b}{\dot{m} C_p}\right) \quad (2)$$

where:

- $T_f = T_{bc}(i)$ Output Temperature of the elevation tube (K)
- $T_{fi} = T_{bd}(i)$ Input Temperature of the elevation tube (K)
- n Number of elevation tubes
- W Width of the absorber plate (m) to the solar collector
- y_b The distance that wants to measure the outlet temperature (m)
- \dot{m} Input mass flow rate (kg/s)
- C_p Specific heat of water (J/kg K)
- T_a Environment Temperature (K)
- S Solar radiation by area of incidence (W / m^2)
- F' The collector efficiency factor
- U_L Overall Coefficient of heat loss in the solar collector (W/m^2K)

Determine the temperature of the water leaving the elevation tube $T_{bc}(i)$, as shown in Fig 3.

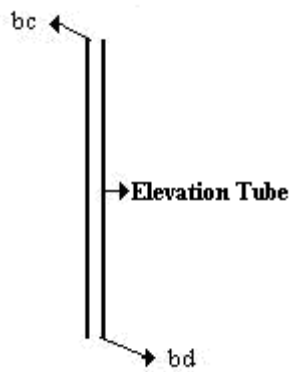


Figure 3. Elevation Tube

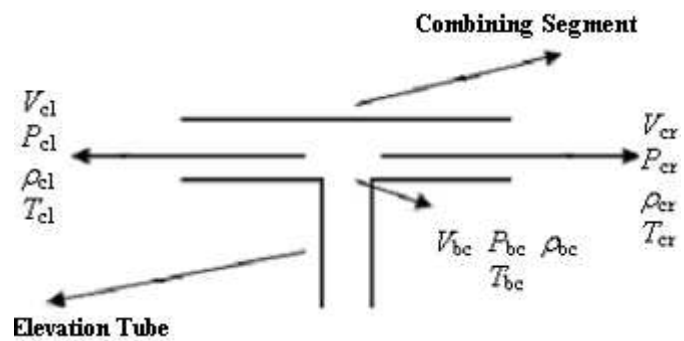


Figure 4. Combining Segment $i = 0$ of the Solar Collector

Calculation of the Collector Overall Heat Loss Coefficient

For a commercial collector without selective surface, the overall coefficient of heat loss is in range: 6.00 to 8.00 (W/m²C). In this work, the following value was adopted:

$$U_L = 6,50 \left(\frac{W}{m^2 C} \right) \quad (3)$$

Calculation of mass flow $\dot{m}(i)$

D_b Diameter of the Elevation tube (m)

$$A_b = \left(\frac{\pi \cdot D_b^2}{4} \right) \quad \text{Area of the elevation tube (m}^2\text{)} \quad (4)$$

$$\rho_{bd}(i) = 999,9 - 0,057 \times T_{bd}(i) - 0,00358 \times T_{bd}(i)^2 \quad \text{Specific Mass (kg/m}^3\text{)} \quad (5)$$

$$\dot{m}(i) = V_{bd}(i) * \rho_{bd}(i) * A_b \quad \text{Mass flow (kg/s)} \quad (6)$$

Calculation of F

Applying the values of the parameters specified for the solar collector used and the physical properties of materials used in the theories of heat transfer and fluid mechanics, the absorber plate efficiency can be calculated from the equation:

$$F = \frac{\tanh \left[\frac{\dot{m}(W - D_b) / 2}{\dot{m}(W - D_b) / 2} \right]}{\dot{m}(W - D_b) / 2} \quad (7)$$

Heat Transfer Relations for Internal Flow - Calculation of h_{fi}

For determination of h_{fi} in the elevation tube, first determine the Reynolds Number from the equation:

$$Re = \frac{V_{bd}(i) \times \rho_{bd}(i) \times D_b}{\mu} \quad (8)$$

where μ : Absolute water viscosity considered constant and equal to 0.001 (kg/m s).

Then determines the Prandtl number of the elevation tube based on the Eq. (9).

$$Pr = \frac{\mu_{\acute{a}gua} \times Cp_{\acute{a}gua}}{k_{\acute{a}gua}} \quad (9)$$

Where:

k Thermal conductivity (W/m K)

Duffie and Beckman (1991) discuss the behavior of mean Nusselt number for small tubes according to the Prandtl number. For the conditions under study, Nusselt is around 5.0. Thus, the value of h_{fi} - Coefficient of heat transfer between the fluid and tube (W/m²K) is given by:

$$h_{fi} = \frac{k_{water} \times Cp_{water}}{D_b} \quad (10)$$

The Efficiency factor of the collector (F') is given by the equation:

$$F' = \frac{1/U_L}{W \left[\frac{1}{U_L} [D_b + (W - D_b)F] + \frac{1}{C_b} + \frac{1}{\pi D_b h_{fi}} \right]} \quad (11)$$

Therefore, determine the outlet temperature of the elevation tube: $T_f = T_{bc}(i)$

Step 3 –Balance of Mass in the elevation tube for the determination of $V_{bc}(i)$

$$V_{bd}(i)\rho_{bd}(i) = V_{bc}(i)\rho_{bc}(i) \quad (12)$$

$$\rho_{bc}(i) = 999,9 - 0,057 \times T_{bc}(i) - 0,00358 \times T_{bc}(i)^2 \quad (\text{kg/m}^3) \quad \text{Specific Mass (kg/m}^3) \quad (13)$$

Step 4 - Balance of mass and energy in the combining segment for the determination of $V_{cr}(i)$ and $T_{cr}(i)$

The diagram corresponding to the combining segment is showed in Fig. 4.

Reapplying the equation of continuity:

$$T_{bc}(i) = T_{cl}(i) \text{ (K)} \quad \text{and} \quad V_{cl}(i) = 0 \text{ (m/s)}$$

Energy equation - Bernoulli

Rewriting the energy equation for the combining segment:

$$A_c \times V_{cl}(i) \times \rho_{cl}(i) \times C_p \times T_{cl}(i) + A_b \times V_{bc}(i) \times \rho_{bc}(i) \times C_p \times T_{bc}(i) + D_b \times D_c \times F' \times [I \times (\tau \times \alpha) - U_L \times (T_{cl}(i) - T_a)] = A_c \times V_{cr}(i) \times \rho_{cr}(i) \times C_p \times T_{cr}(i) \quad (14)$$

Based on the balance equations of mass and energy, it was determined $V_{cr}(i)$ and $T_{cr}(i)$. It should be noted that for the combining segment accepts a Internal heat transfer coefficient of $h_{fi} = 300$ (W/m²K) (Duffie and Beckamn, 1991). Obtained, therefore, an efficiency factor F' . This value will be accepted for all combining segments in all nodes due to the fact it represents a mean coefficient of heat transfer for this segment. Where: D_c Diameter of the combining manifold (m), A_b area of the elevation tube (m) and $V_{bc}(i)$ output speed of the elevation tube (m/s).

$$A_c = \frac{(\pi \times D_c^2)}{4} \quad \text{Area of the Combining Manifold (m}^2) \quad (15)$$

$$\rho_{cr}(i) = 999,9 - 0,057 \times T_{cr}(i) - 0,00358 \times T_{cr}(i)^2 \quad (\text{kg/m}^3) \quad \text{Specific Mass (kg/m}^3) \quad (16)$$

$$\rho_{cl}(i) = 999,9 - 0,057 \times T_{cl}(i) - 0,00358 \times T_{cl}(i)^2 \quad (\text{kg/m}^3) \quad \text{Specific Mass (kg/m}^3) \quad (17)$$

Step 5 - Momentum Equation in the dividing segment for determination of $P_{dr}(i)$

Applying the momentum equation for the conditions:

$$P_{dl}(i) - P_{dr}(i) = C_d (\rho_{dr}(i) V_{dr}(i)^2 - \rho_{dl}(i) V_{dl}(i)^2) + K_1 (\rho_{dr}(i) V_{dr}(i)^2 + \rho_{dl}(i) V_{dl}(i)^2) \quad (18)$$

$$P_{dl}(i) = 101325 \times \left(1 - \frac{0,0065 \times 850}{288,16} \right) \left(\frac{9,807}{287 \times 0,0065} \right) \quad (19)$$

Where: $V_{dl}(i)$ input speed in the dividing segment (m/s), $T_{dl}(i)$ input temperature in the dividing segment (K), $T_{dr}(i)$ output temperature in the dividing segment (K), $V_{dr}(i)$ output speed in the dividing segment (m/s), $P_{dl}(i)$ input pressure in the dividing segment (N/m²) and $P_{dr}(i)$ output pressure in the dividing segment (N/m²).

$$\rho_{dl}(i) = 999,9 - 0,057 \times T_{dl}(i) - 0,00358 \times T_{dl}(i)^2 \quad (\text{kg/m}^3) \quad \text{Specific Mass (kg/m}^3) \quad (20)$$

$$\rho_{dr}(i) = 999,9 - 0,057 \times T_{dr}(i) - 0,00358 \times T_{dr}(i)^2 \quad (\text{kg/m}^3) \quad \text{Specific Mass (kg/m}^3) \quad (21)$$

The Water Flow in pipes - determination of K_1 :

Assuming: D_d Diameter of the dividing segment (m) and D_b diameter of the elevation tube (m), the Eq. (22) gives K_1 :

$$K_1 = 0,42 \left(1 - \frac{D_d^2}{D_b^2} \right) \quad (\text{Pressure Loss Coefficient}) \quad (22)$$

For the determination of C_d (Correction factor of the flow momentum), it is necessary to define preliminarily the type of regime, laminar or turbulent and will not be show in this text.

Step 6 - Momentum Equation in the elevation tube and combining segment to determine the $P_{bc}(i)$, $P_{bd}(i)$

Applying the momentum equation for the elevation tube:

$$(P_{bd}(i)) - (P_{bc}(i)) = \left[f \frac{(H - 0,5 \times D_b - 0,5 \times D_c)}{D_b} + K_b \right] \times \rho_{bd}(i) V_{bd}(i)^2 + (\rho_{bd}(i) + \rho_{bc}(i)) \times g \times H \times \text{sen}(\theta) \quad (23)$$

$$P_{bd} = \frac{(P_{dl} + P_{dr})}{2} \quad (24)$$

The friction factor is given by the Eq. (25):

$$f = \frac{64}{Re} \quad \text{Assuming:} \quad K_b = 12,94 \quad (\text{Pressure Loss Coefficient into the elevation tube}) \quad (25)$$

Where: $V_{bd}(i)$ Input speed in the elevation tube (m/s), g Acceleration of gravity (m/s²), θ Inclination angle of the collector and P_{bd} and P_{bc} are the input and output pressure into the elevation tube (N/m²).

Step 7 - Visualization of pressures, speeds and temperatures in the node $i = 0$

Figure 5 shows the discretization of the pressure, velocities and temperature values at node $i = 0$, for the dividing and combining segments and elevation tube.

Step 8 - Resolution of the equations that govern the transition from node $i = 0$ to the node $i = 1$

Completed the calculations for the node $i = 0$ is necessary to make the transition to the next node $i = 1$, as showed at the Fig. 6. This transition is based on the equations of mass conservation, momentum and conservation of energy. These equations together allow to obtain the output velocities, temperatures and pressures in the dividing and combining manifolds. These variables represent the initial data to obtain the results for the node $i = 1$ (Cooper and Dunkle, 1981).

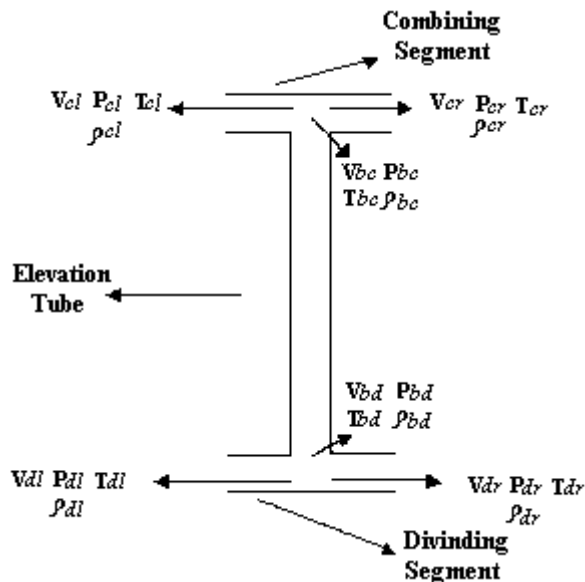


Figure 5. Node $i = 0$ completed

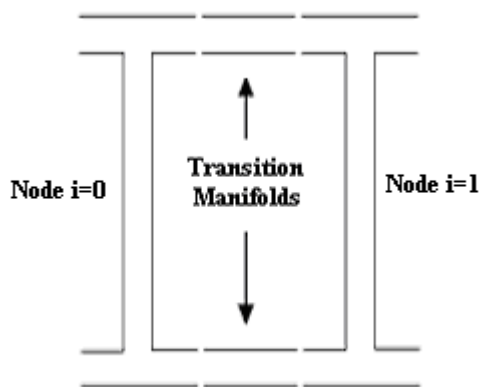


Figure 6. Transition from the node $i = 0$ to $i = 1$

3. EXPERIMENTAL PROCEDURE

3.1. Test for thermal and flow evaluation in solar collector plans

The experiments were conducted on internal testing bench of solar collectors in operation in the Group for Research in Energy (GREEN) of PUC Minas and aim to evaluate the thermal performance of a plan solar collector for different levels of water flow, including the measure of the pressure loss through the collector for each test condition. The results will be used to experimentally validate the numerical model developed in the scope of this work. The solar collector has been tested by European Standard prEN 12975-2: Thermal Solar Systems and Components - Solar Collectors - Part 2: Test Methods, including measurements of pressure at the entry and exit of the solar collector and variable water flow. Unlike the European standard adopted, were defined 09 ranges of flow that vary from $8.67 \times 10^{-6} \text{ m}^3/\text{s}$ to $7.73 \times 10^{-6} \text{ m}^3/\text{s}$ for water through the solar collector.

4. DISCUSSIONS OF EXPERIMENTAL AND NUMERICAL RESULTS

4.1. Temperatures Distribution in the solar collector

The analysis with the temperature distribution in the solar collector to validate the model was developed comparing the results of numerical simulation with those obtained experimentally. Should be clear that the simulation proposed in the scope of this project estimated the temperature of the fluid working in various positions of the solar collector, while obtained through the experimental procedure are the temperatures on the surface of the absorber plate, with the exception of the entry and exit temperatures of the collector, which are measured directly. In numerical simulation, was used as input data the experimentally measured values for temperature and water flow into the collector, environment temperature, wind speed and solar radiation. Figure 7 summarizes the numerical and experimental results. There is a good agreement between these temperatures for the fluid by calculating the combined uncertainty for each measure depending on the temperature of the fluid flow. These values are between 273.3 and 273.24 K. A further analysis to be made is about the magnitude of the temperature in the experimental procedure on the numerical model. As already stated above, the model proposed here shows the temperatures of the working fluid, while the experimental procedure were the measurements of temperatures on the surface of the absorber plate. So we can conclude that a good part of the energy provided by solar radiation is not transferred to the fluid, causing differences between those from 280.15 to 287.15 K between the water and the plate.

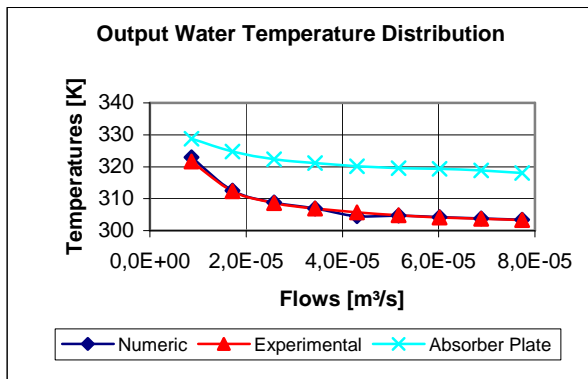


Figure 7. Output Water Temperature Distribution

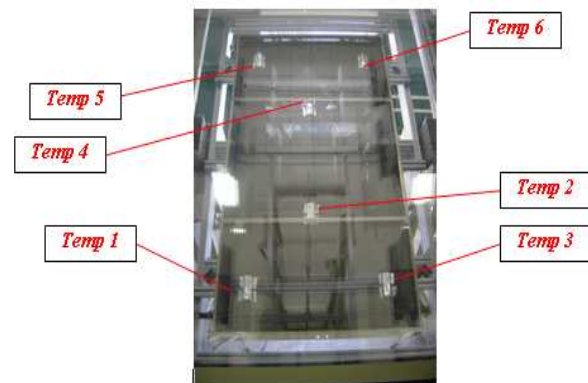


Figure 8. Setting of thermocouples in the absorber plate.

This difference is expected in the model discussed by Duffie and Beckmann (1991) by means of heat removal factor F_R , shows that these differences are inherent in the manufacture of the collector and the operating conditions. Thus, it was expected that for higher flow rates the difference between the temperatures of the plate and fluid is increasingly smaller. In the limit, for infinitely high flows, the plate and the fluid have the same temperature. However, in this work, we observed the opposite. Thus, the experimental tests were performed again, now with the attachment of thermocouples in the back (shaded surface) of the absorber plate. This change was suggested, because despite the care taken in the first assembly, it was necessary to assess the possible influence of radiation incident on the thermocouples. The results are repeated. A plausible explanation for this fact can be attributed to non-uniform flow distribution in the elevation tubes.

4.2. Qualitative evaluation of the flow distribution in the solar collector

To validate the numerical model for the flow distribution through the collector (elevation tubes and dividing and combining manifolds) was proposed a test for indirect flow evaluation at each point. This procedure was adopted, seeking to reduce costs and inherent complexity in the direct method that requires the setting of individual water flow meters in each segment of the pipeline and each elevation tube. The alternative adopted deals with the temperatures measurement over the plate absorbers segments to spatial behavior evaluation of the water flow through the solar collector. The correlation of these two variables is reversed, because the points of higher temperature correspond to places of lower water flows. Figure 8 shows the points of attachment of the thermocouples in the absorber plate.

The methodology for flow distribution evaluation along the dividing and combining manifolds and elevation tubes will be conducted for each flow range specified. Furthermore, it is important to make the following distinction. The thermocouples to determine the temperatures of the plate at the entrance and the exit of the dividing manifold are: Temp 1 (Input) and Temp 3 (Output). For the combining manifold the thermocouples are: Temp 5 (Input) and Temp 6 (Output). All sensors together will be evaluated to determine the temperature profile of the distribution pipes. All temperatures were experimentally collected on the plate absorber, while the temperatures obtained in the mathematics simulation correspond to the fluid temperature. Therefore, the analysis is expected to follow a temperature difference between the experimental (absorber plate) and the numerical temperature (fluid).

4.2.1. Temperature Distribution along the dividing and combining manifolds

Analyzing the experimental results for the dividing e combining manifolds are observed that in all the flow ranges, there was an increase in the plate temperature characterized by reduction of the difference (Temp 3 - Temp 1 and Temp 6 - Temp 5) measures along the manifolds. There is also that for higher flow rates the difference in temperature is reduced. This behavior was expected and indicates the transfer of useful heat to water in this region and decrease of the flow along the dividing manifold. As the discrepancy founded for the thermocouples measures are within the range of combined uncertainty, the results for the dividing manifold, summarized in Fig. 9, are quite satisfactory with a maximum difference between numerical and experimental values is nearly 1.25 K to the flow of $8.67 \times 10^{-6} \text{ m}^3/\text{s}$ and a minimum difference of 0.25 K for flow rates above $7.6 \times 10^{-5} \text{ m}^3/\text{s}$. Analyzing the results for the flow behavior in the combining manifold, there was again a good agreement between theoretical and experimental values. As the discrepancy founded for the thermocouples measures are within the range of combined uncertainty, the temperature behavior in combining manifold, comparing the numerical and experimental results, are quite satisfactory. The best result was in the flow rate of $4.3 \times 10^{-5} \text{ m}^3/\text{s}$ with a deviation between the numerical and experimental results of only 0.05 K, while the largest deviation occurred for the flow of $8.67 \times 10^{-6} \text{ m}^3/\text{s}$ and was about 1.38 K. Figure 10 summarizes the results for the combining manifold.

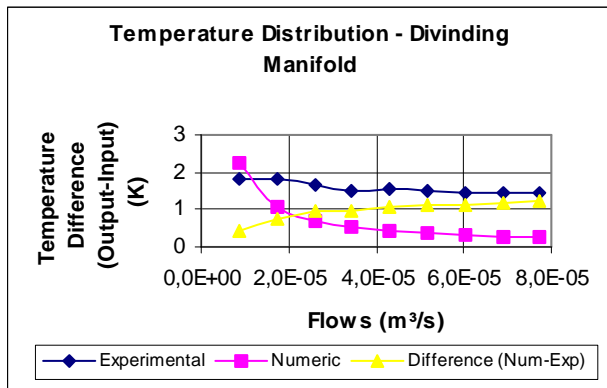


Figure 9. Temperature distribution-dividing manifold

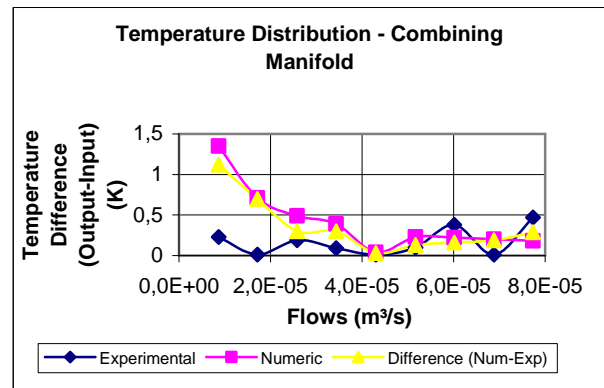


Figure 10. Temperature distribution-combining manifold

4.2.2. Temperature distribution in the elevation tubes

First, it should adopt the following criterion: The sensors Temp 1 and Temp 5 represent the temperature distribution along the first elevation tube of the solar collector. Sensors Temp 2 and Temp 4 represent the temperature distribution along the intermediary elevation tube. Sensors Temp 3 and Temp 6 represent the temperature distribution in the last elevation tube. The analysis will be only for the last and intermediate elevation tubes, because it is where are the best and worst results. The same procedure adopted for the dividing and combining manifolds can be used for the elevation tubes. First, it is observed for the last elevation tube was evaluated the difference of the temperature between the output (input of the combining manifold) and input (output of the dividing manifold). It is natural that there is a difference between numerical and experimental results, as mentioned before the experimental results report the temperature on the surface of the absorber plate, while the numerical results inform the temperature of the fluid itself. The results are shown in Figure 11. However, what is evaluated here is the results behavior of the temperatures in the experimental procedure and numerical simulation in order to validate the model. Evaluating all the elevation tubes together, it appears that the model works better in the flow rate range of $7.73 \times 10^{-5} \text{ m}^3/\text{s}$ with a deviation between numerical and experimental results of 1.89 K and lower in the range of $8.67 \times 10^{-6} \text{ m}^3/\text{s}$ with a deviation of 9.47 K.

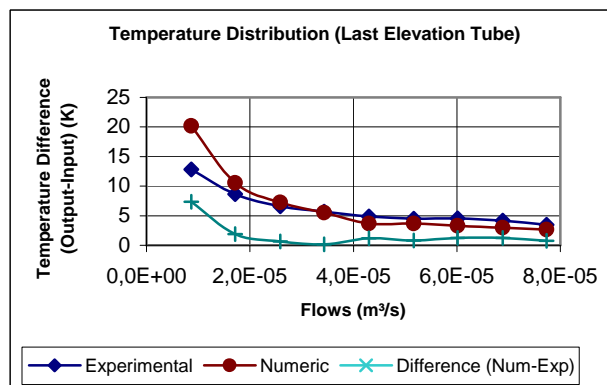


Figure 11. Temperatures in the last elevation tube

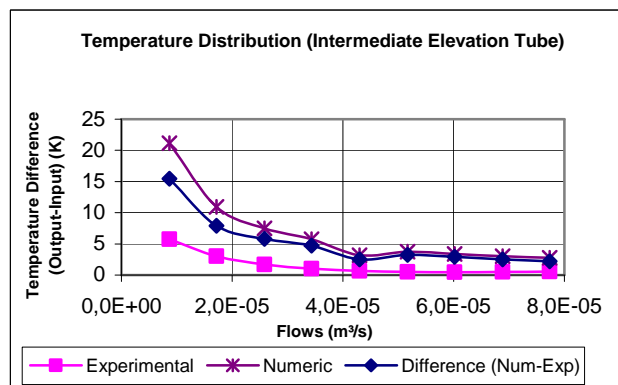


Figure 12. Temperature in the intermediate elevation tube

The highest average variation among the differences (Experimental and Numerical) occurs in the intermediate elevation tubes and is approximately 15.43 K as shown in Fig. 12. This is very significant for a flat plate solar collector. However, there are two possible reasons for this phenomenon. The first is that the position of thermocouples in the intermediate elevation tubes is different to those elevation tubes at the periphery and therefore generates an error on this scale. The other factor, which in fact is more likely to justify what happened, is that the model of flow distribution (Hardy Cross) proposed in the course of this work does not represent the most appropriate profile of the flow in the elevation tubes. There are several publications on the subject, the most recent was developed by Cardoso (2007) which presents a methodology based on numerical simulation using the software CFX - 10 (Numerical Simulation Software) preventing their application in batteries of solar collectors. The author comes to profiles of flow in the elevation tubes that do not resemble the symmetrical model developed here. However, for the dividing and combining manifolds the flow behavior proposed by Cardoso (2007) is approaching in a reasonable manner. Finally concludes that the model proposed here, for the flow distribution in a solar collector (dividing and combining manifolds and elevation tubes),

operates in a coherent way for the dividing and combining manifolds in flow rates equal and/or higher than 3.43×10^{-5} m³/s. For intermediate elevation tubes, the model not produced good results in comparison with the experimental results and the model proposed by Cardoso (2007), however, for a initial view of the flow distribution, the developed model is satisfactory and gives good results when used for flow rates above 3.33×10^{-5} m³/s.

4.2.3. Pressure distribution in the solar collector

For simplicity, the study is shown only for the flow of 3.43×10^{-5} m³/s, for other flows, the behavior is similar. For experimental determination of the pressure loss in the solar collector were fixed two pressure transducers, the first located at the entrance of the solar collector and the second to exit of the water in the solar collector. Thus, through the experimental procedure, were obtained only the pressure values at entry and exit of the collector, the intermediate pressure were simulated numerically. The pressure loss measured during the experimental procedure was approximately 5.88×10^{-3} bar, while the numerical simulation was approximately 2.15×10^{-3} bar. Thus was obtained a difference between the experimental procedure and numerical simulation of 3.73×10^{-3} bar. In a solar collector, where the losses for this flow arriving at the most 7.84×10^{-3} bar, it was concluded that there is a very significant error between the numerical and experimental results. One solution to the problem is to repeat the test with stronger connections to the sensors.

5. CONCLUSIONS

Based on the theory described in the course of this work and the experimental results, it was concluded that the proposed mathematical model, based on the laws of mass conservation, energy and momentum, reaching good results for flows greater than or equal to 3.43×10^{-5} m³/s (flow allowed by the test standard for a collector area of 1.72 m²). Highlights that for installations of solar heating in forced circulation, the recommended flow rates are equal or even 20% higher than the flow test, the region, where the model has better performance. The temperature distribution, pressure and flow through the collector showed to be consistent with the various work done in this area. The non-uniformity of water flow along the collector and its influence on the water output temperature has been demonstrated numerically and experimentally and compared with the literature. The results demonstrate the need for a more careful examination on the Hardy Cross model for initialization of the flow rates values. It was noted that some variables, such as the level of penetration of the elevation tubes in the manifolds, previously had been neglected with the justification of not being relevant to a numerical analysis. However, it was observed that the variable in question is of significant importance in the results for the flow and temperature distribution when measured at high flow rates ($> 7.73 \times 10^{-5}$ m³/s), besides the pressure loss. The experimental methodology used was conducted in internal testing with the Solar Simulator of the Study Group on Energy (GREEN), in this equipment, variables such as solar radiation, temperature and wind speed are kept almost uniform during the tests. The results obtained experimentally were compared with the numerical ones, considering tolerances and uncertainties of the instrumentation used to obtain significant results on the simulation results especially for the distribution of the fluid temperature.

6. ACKNOWLEDGEMENTS

Thanks to the Studies and Projects' Financier (FINEP) for financial support

7. REFERENCES

- Cardoso, R., 2007, "Avaliação numérica do escoamento em um coletor solar", Solar Energy Brazilian Congress .
- Chiou J. P., 1982, "The effect of nonuniform fluid flow distribution on the thermal performance of solar collector", Solar Energy, Vol. 29, No. 6, pp. 487-502.
- Cooper, P. I. and Dunkle V., 1981, "A non-linear flat-plate collector model", Solar Energy, Vol. 26, pp. 133-140.
- Duffie, J. A. and Beckman, W. A., 1991, "Solar Engineering of Thermal Processes", Second Edition.
- Kang, M.C., Kang Y.H., Lim, S.H., Wongee C., 2006, "Numerical analysis on the thermal performance of a roof integrated flat-plate solar collector assembly", International Communications in Heat and Mass Transfer.
- Oliva, A., Costa, M., and Perez, S. C. D., "Numerical simulation of solar collectors: the effect of nonuniform and nonsteady state of the boundary conditions", Solar Energy, Vol. 47. No. 5, pp. 359-373.
- Simon, F. F., "Flat-plate solar-collector performance evaluation with a solar simulator as a basis for collector selection and performance prediction", Solar Energy, Vol. 18, pp. 451-466, 1976.
- Wang, X. A. and Wu, L. G., 1990, "Analysis and performance of flat-plate solar collector arrays", Solar Energy, Vol. 45, No. 2, pp. 71-78.

8. RESPONSIBILITY NOTICE

The authors are the only responsible for the printed material included in this paper.